

Research Article

Antigenic and Genotypic Similarity between Primary Glioblastomas and Their Derived Neurospheres

Valentina Caldera,¹ Marta Mellai,¹ Laura Annovazzi,¹ Angela Piazzini,^{1,2} Michele Lanotte,³ Paola Cassoni,⁴ and Davide Schiffer¹

¹Neuro-Bio-Oncology Center, Policlinico di Monza Foundation, University of Turin, 13100 Vercelli, Italy

²Department of Medical Sciences, University of Piemonte Orientale, 28100 Novara, Italy

³Department of Neuroscience, Neurosurgical Unit, University of Turin, 10124 Turin, Italy

⁴Department of Biomedical Sciences and Human Oncology, University of Turin, 10124 Turin, Italy

Correspondence should be addressed to Davide Schiffer, davide.schiffer@unito.it

Received 14 February 2011; Revised 4 April 2011; Accepted 6 June 2011

Academic Editor: Dominic Fan

Copyright © 2011 Valentina Caldera et al. This is an open access article distributed under the Creative Commons Attribution License, which permits unrestricted use, distribution, and reproduction in any medium, provided the original work is properly cited.

Formation of neurospheres (NS) in cultures of glioblastomas (GBMs), with self-renewal, clonogenic capacities, and tumorigenicity following transplantation into immunodeficient mice, may denounce the existence of brain tumor stem cells (BTSCs) *in vivo*. In sixteen cell lines from resected primary glioblastomas, NS showed the same genetic alterations as primary tumors and the expression of stemness antigens. Adherent cells (AC), after adding 10% of fetal bovine serum (FBS) to the culture, were genetically different from NS and prevalently expressed differentiation antigens. NS developed from a highly malignant tumor phenotype with proliferation, circumscribed necrosis, and high vessel density. Beside originating from transformed neural stem cells (NSCs), BTSCs may be contained within or correspond to dedifferentiated cells after mutation accumulation, which reacquire the expression of stemness antigens.

1. Introduction

In leukemias, rare tumor cells show extensive proliferative and self-renewal potential and are responsible for maintaining the tumor clone [1]; similar cells were subsequently described in gliomas [2–4]. They were called brain tumor stem cells (BTSCs), believed to be responsible for tumor growth, recurrence and resistance to therapies and, supposedly, to derive from neural stem cells (NSCs) transformation and to be related to restricted unipotent or multipotent progenitors [5–7]. They share with NSCs antigenic properties of stemness, such as Nestin, Musashi-1, CD133, and SOX2 expression [8]; it has been suggested to better identify them on the basis of their functional competence than as cell types [9]. A derivation from dedifferentiated tumor cells that reacquire stem cell-like properties has also been hypothesized [3, 10, 11].

Beside common antigenic properties with NSCs, BTSCs share genetic properties with primary tumor cells. Their existence in tumors is indirectly demonstrated by the generation,

from tumor samples put in culture, of neurospheres (NS) and, by adding 10% of fetal bovine serum (FBS), of adherent cells (AC) with different capacities of self-renewal, differentiation, clonogenicity, and tumorigenicity. The demonstration of BTSCs *in vitro* may be influenced by the methodological procedures employed and may have different expression modalities [12, 13]. For example, using N29 and N32 tumor models, it has been demonstrated that NS formation is not necessary to enrich for tumorigenic cells, due to the fact that AC can display high clonogenicity *in vitro*, tumorigenicity *in vivo*, and high expression of CD133 and Nestin [14].

Recently, two transcription factors have been proposed as putative markers of stemness: sex determining region of Y chromosome (Sry)-related high mobility group box2 (SOX2) and repressor element-1 silencing transcription/neuron-restrictive silencer factor (REST/NRSF). SOX2 belongs to a family of transcription factors expressed in the central nervous system (CNS) at early stages of development [15] and it is expressed in malignant gliomas at both mRNA and

TABLE 1: List of antibodies.

Antibody	Source	Dilution IHC	Dilution WB	Code	Company
Nestin ^{*,°}	Mouse	1 : 200	—	MAB5326	Chemicon
Nestin ^{*,°}	Rabbit	1 : 200	1 : 1000	AB5922	Chemicon
GFAP [°]	Mouse	1 : 200	—	M0761	DakoCytomation
GFAP [°]	Rabbit	1 : 200	1 : 1000	Z0334	DakoCytomation
CD133 [°]	Mouse	1 : 20	1 : 250	130-090-422	Miltenyi Biotec
Musashi-1 [°]	Rabbit	1 : 200	1 : 500	AB5977	Chemicon
SOX2 ^{*,°}	Rabbit	1 : 50	—	sc-20088	Santa Cruz Biotech.
SOX2 ^{*,°}	Mouse	1 : 100	1 : 250	MAB2018	R&D Systems
REST ^{*,°}	Rabbit	1 : 150	—	IHC-00141	Bethyl Laboratories
REST	Rabbit	—	1 : 2500	A300-540A	Bethyl Laboratories
GalC ^{*,°}	Mouse	1 : 200	—	MAB342	Chemicon
β III-Tubulin ^{*,°}	Mouse	1 : 250	—	MAB1637	Chemicon
Ki-67/MIB-1 [*]	Mouse	1 : 100	—	M7240	DakoCytomation
MGMT	Mouse	—	1 : 400	MS-470-P0	Lab Vision Corp.
α -Tubulin	Rabbit	—	1 : 5000	LF-PA0146	LabFrontier
CD34	Mouse	Pre-diluted	—	790-2927	Ventana

* HIER required.

° Tested by IF.

protein level [16]. The second putative marker is REST/NRSF (REST), which represses transcription of several neuronal genes by binding to a DNA regulatory motif known as repressor element 1/neuron-restrictive silencer element (RE1/NRSE) [17]. REST is highly expressed in NSCs and its transcription is blocked as they exit the cell cycle and differentiate [18].

There is no possibility to demonstrate the existence of BTSCs in tumors before surgical intervention as to be useful for therapeutic strategies. Specific phenotypes have been shown to be related with the derivation of NS from surgical samples [19, 20], but it has not yet been definitively established whether the phenotypical heterogeneity influences [21] or not [22] the occurrence of BTSCs.

In a series of GBMs we wanted to verify from the genetic and antigenic point of view the relationship between NS with AC and the primary tumor phenotype.

2. Materials and Methods

2.1. Patients. The investigation was carried out on 16 partially resected primary hemispheric GBMs (CV1-20) operated on at the Department of Neuroscience, Neurosurgical Unit, University of Turin. Histological diagnosis of GBM was performed according to WHO guidelines [23]. The mean age of the patients was 62 years (range: 23–76 years). Ten patients were males, and 6 were females.

The patient stratification was as follows: out of 16 GBM patients, 10 received postoperative standard radiation therapy (RT) (60 Gy total dose in 27–30 fractions administered via a LINAC). Among the 10 irradiated patients, 8 received standard Temozolomide (TMZ) therapy (75 mg/m²/daily for 6 weeks), followed by adjuvant TMZ (200 mg/m² from day 1 to day 5 every 4 weeks for 6–12 cycles). Two patients received TMZ, but no radiation therapy. Of the remaining patients,

2 did not receive any treatment because of low Karnofsky Performance Status (KPS), and 2 were lost at follow up. All patients are still alive with the exception of 2 patients who died 3 months following surgery.

A viable sample from the dissected tumor was divided into three serial slices: one was stored at –80°C for molecular genetics and frozen sections, one was fixed in buffered-formalin and embedded in paraffin (FFPE) and one was washed, minced, and enzymatically dissociated for expansion in culture. A peripheral blood sample was obtained from each patient and was stored at –20°C. All patients provided informed consent allowing for the use of tumor specimens for molecular and cell culture studies. The study was approved by the Ethics Committee of the University Hospital of Turin.

2.2. Histology, Immunohistochemistry (IHC), and Immunofluorescence (IF). Haematoxylin and eosin stain (H&E) was performed on 4 μ m paraffin sections.

IHC was performed on 4 μ m paraffin sections using a Ventana Full BenchMark automatic immunostainer (Ventana Medical Systems Inc., Tucson, AZ, USA). UltraView Universal DAB Detection Kit was used as detection system. The antibodies used are listed in Table 1. Heat-induced epitope retrieval (HIER) was performed in Tris-EDTA, pH 8 (Ventana Medical Systems). Negative controls were obtained by omitting the primary antibody.

Double immunohistochemistry was performed using Nestin, GFAP, and CD34 antibodies with ultraView Universal Alkaline Phosphatase Red Detection Kit as chromogen (Ventana Medical Systems).

IF was performed on frozen sections, NS and AC. Goat anti-rabbit FITC-conjugated IgG and rabbit anti-mouse TRITC-conjugated IgG antibodies were used. Cell nuclei were stained with DAPI. The antibodies used are listed in Table 1. Observations were made on a Zeiss Axioskop

TABLE 2: Microsatellites markers used for LOH analysis.

Region	STR	Locus	Repeat	Max. het*	PCR primers 5' to 3 (forward/reverse)
1p	D1S508	1p36.23	(AC) _n	0.812	AGCTGGGGAATATATGTNTCATATTGTGGAAGGCCAACTC
	D1S496	1p36.1-p34.3	(AC) _n	0.815	TCTCTATGCATCTATGCATCTATCTGCATTTGTCTGGGTTCTT
	D1S2724	1p33	(AC) _n	0.821	TCAAGTCCCAGGAGGATTCCACTGTGTTATTTAGCAGGAT
	D1S457	1p13.3	(AC) _n	0.742	GGGGGCAATAACACAAAGGAGCCTGGAGCCAAGAGTGCTA
9p	D9S157	9p22.2	(AC) _n	0.849	AGCAAGGCAAGCCACATTTCTGGGGATGCCAGATAACTATATC
	D9S171	9p21.1	(AC) _n	0.804	AGCTAAGTGAACCTCATCTCTGTCTACCCTAGCACTGATGGTATAGTCT
	D10S212	10q26.3	(AC) _n	0.74	GAAGTAAAGCAAGTTCTATCCACGGAAGTAAAGCAAGTTCTATCCACG
10q	D10S190	10q26.11	(AC) _n	0.863	GTGTTTGGGTCATGGAGATGAGGCAAAGCAGGAGCA
	D10S562	10q25.3	(AC) _n	0.715	CCTGGCAGATGGAGGTTTCGGAGTGCTTCCTTAAATAC
	TP53 Alu	17p13.1	(AAAAT) _n	0.594	ACTCCAGCCTGGGCAATAAGAGCTACAAAACATCCCCTACCAAACAGC
17p	D17S520	17p13	(AC) _n	0.854	GGAGAAAAGTGATACAAGGGATAGTTAGATTAATACCCACC
	D19S412	19q13.33	(AC) _n	0.812	TGAGCGACAGAATGAGACTACATCTTACTGAATGCTTGC
19q	D19S219	19q13.32	(AC) _n	0.77	GTGAGCCAAGATTGTGCCGACTATTTCTGAGACAGATTCCCA

STR: Short Tandem Repeat.

*Maximum heterozygosity.

fluorescence microscope (Karl Zeiss, Oberkochen, Germany) equipped with an AxioCam5MR5c and coupled to an Imaging system (AxioVision Release 4.5, Zeiss).

2.3. In Vitro Cultures. Tumor tissue was processed as previously described [24]. Culture conditions were the following: for NS, Dulbecco's modified Eagle's medium (DMEM)/F-12 with 10 ng/mL bFGF (basic fibroblast growth factor) and 20 ng/mL EGF (epidermal growth factor); for AC, DMEM with 10% fetal bovine serum (FBS). Both cultures were maintained at 5% O₂/CO₂. GBM reference cell lines were U87-MG and 010627 (Galli R, DIBIT San Raffaele, Milan) for both AC and NS.

All cell cultures were periodically checked for *Mycoplasma* contamination (e-Myco Mycoplasma PCR Detection kit, iNtRON Biotechnology, Korea).

For population analyses, cells were plated at 200,000 cells/cm², and the resulting spheres were collected every 4–6 days. The total number of viable cells was assessed at each passage by Trypan blue (Sigma, St. Louis, MO, USA).

Clonogenic assays were performed as previously described [25]. Briefly, NS were dissociated into single cells and plated into a 96-well plate for the subsphere-forming assay by limiting dilution. Single-cell suspensions were diluted and plated at 1–2 cells/well. After plating, cells were monitored, and only wells containing a single cell were considered for the analysis. Wells were scored for sphere formation following one month of culture.

Differentiation assays were performed by mitogen withdrawal and the addition of 3% FBS to the culture.

2.4. Tumorigenicity. It was tested by transplanting NS and AC from each sample into *NOD SCID* mice (Charles River, Calco, Italy). Two microliters of a 1×10^8 cells/mL suspension were stereotactically injected into the right striatum according to the procedure described in Galli et al. [3]. Mouse brains were treated with FFPE using the same procedures as

described for primary tumors. Injections were carried out at the H. S. Raffaele, Milan.

2.5. Ethics Statement. All animals were handled in strict accordance with good animal practice as defined by the relevant international (Directive 86/609/EEC and recommendation 2007/526/EC from the European community) and national (Legislative Decree 116/92 and law n. 413/1993) directives and according to protocols approved by the Animal Care and Use Committee of the H. S. Raffaele (IACUC #316).

2.6. DNA Extraction. Genomic DNA was extracted from frozen tumor samples according to a standard phenol-chloroform protocol. DNA extraction from cell lines was performed with the QIAmp DNA Mini Kit (Qiagen GmbH, Hamburg, Germany) and from peripheral blood by a salting-out procedure. The genetic analyses described below were carried out on primary tumors, NS and AC.

2.7. Loss of Heterozygosity (LOH) Analysis. Allelic imbalances were determined by LOH analyses of microsatellite markers. Highly polymorphic markers were selected based on their heterozygosity and position on the five most frequently deleted chromosomes in gliomas (Table 2). Microsatellites were amplified in multiplex reactions by PCR with fluorescently labeled primers (Applied Biosystems). Amplification was performed with a standard touchdown protocol. Following electrophoresis on an ABI 3130 Genetic Analyzer (Applied Biosystems), data were collected by GeneMapper v4.0 software (Applied Biosystems). LOH was determined by measuring the peak height ratio between the two alleles (allelic ratio) in constitutive (N1/N2) and tumor (T1/T2) DNA samples. Allelic imbalance was calculated from the ratio of N1/N2 to T1/T2. Values less than 0.5 and greater than 1.5 were considered evidence of LOH [26].

2.8. EGFR Amplification Status. As in previous studies, EGFR amplification status (GeneBank sequence NM_005228) was

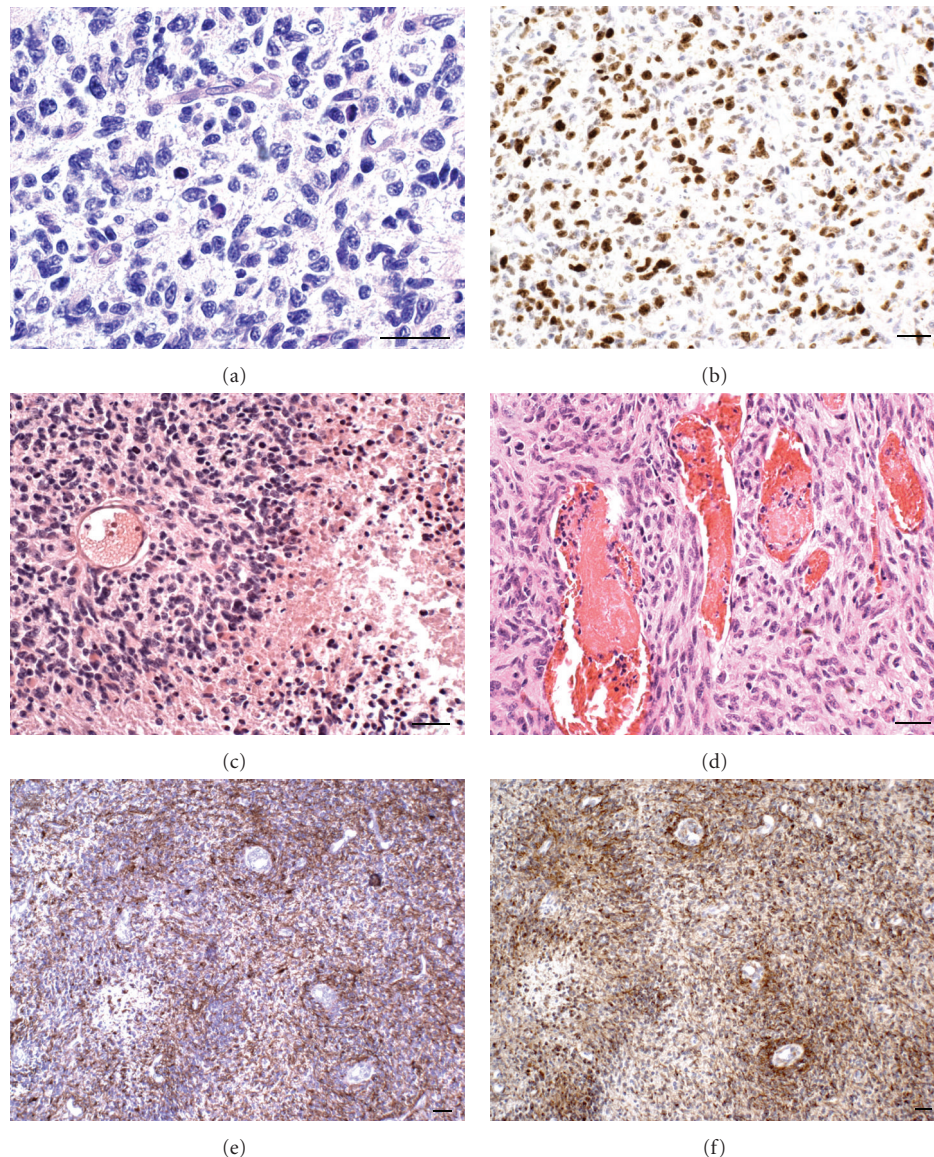


FIGURE 1: Histological and immunohistochemical aspects of phenotypic areas from which NS and AC generated. (a) High cell density, nuclear pleomorphism, scanty cytoplasm, and visible mitoses, H&E. (b) High Ki-67/MIB.1 LI, DAB. (c) The external slope of a circumscribed necrosis, H&E. (d) High vessel density, H&E. (e) Hypercellular perivascular cuffings. GFAP is more positive than Nestin (f), DAB. Scale bar 50 μ m.

assessed by Fragment Analysis and Capillary Electrophoresis (CE) on an ABI 3130 Genetic Analyzer (Applied Biosystems, Foster City, CA, USA). $\text{INF-}\gamma$ was used as reference house-keeping gene. The amplification status of the EGFR gene was determined by measuring the EGFR/ $\text{INF-}\gamma$ ratio. A ratio greater than 2.09 was considered evidence of more than two copies of the EGFR gene.

2.9. MGMT Promoter Hypermethylation Status. MGMT promoter hypermethylation status (GeneBank sequence NM_002412) was determined by Methylation Specific Polymerase Chain Reaction (MS-PCR) followed by CE as previously reported [27]. Sodium bisulfite modification was performed with the MethylEasy DNA Bisulphite Modification Kit (Human Genetic Signatures Pty Ltd, Macquarie Park, Sydney,

Australia) [27]. CpGenome Universal Methylated DNA (Chemicon International Inc., Temecula, CA, USA), and normal lymphocyte DNA samples were used as methylated and unmethylated controls, respectively. Primer sequences for MS-PCR and amplification conditions were previously reported [28]. Following electrophoresis using an ABI 3130 Genetic Analyzer (Applied BioSystems), data were collected by the GeneMapper Software v4.0 for fragment analysis (Applied BioSystems). The peak height ratio between peaks for the methylated and unmethylated allele was determined. Values greater than 0.1 were scored as evidence of the methylated status of the MGMT gene.

2.10. TP53, PTEN, EGFR, IDH1, and IDH2 Mutation Analysis. The entire coding region of PTEN (exons 1–9)

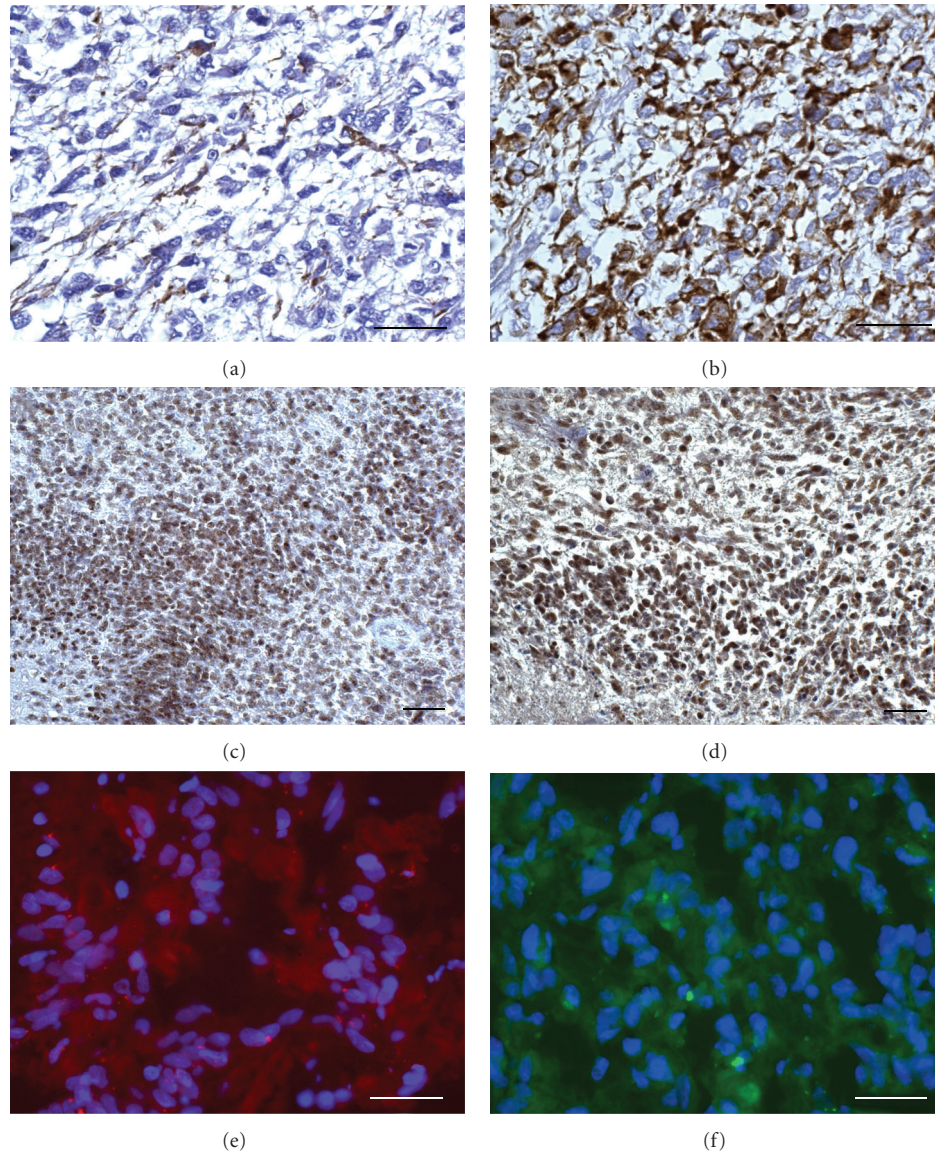


FIGURE 2: Immunohistochemistry of a parallel section of Figure 1. (a) Poor GFAP expression. (b) High Nestin expression. (c) SOX2 is highly expressed in nuclei of the external slope of circumscribed necrosis. (d) REST expression, all DAB. (e) CD133-positive area, frozen section. (f) Musashi-1-positive area. Scale bar 50 μ m.

(GeneBank sequence NM_000314) and TP53 (exons 1–11) (GeneBank sequence NM_000546), the tyrosine kinase domain (TK) (exons 18–24) of EGFR (GeneBank sequence NM_005228), and codons R132 of IDH1 (GeneBank sequence NM_005896) and R172 of IDH2 (GeneBank sequence NM_002168) were investigated for variations by direct sequencing. A minimum of 50 bp of each flanking intronic sequence was also analyzed. All fragments were amplified by PCR using a standard touchdown protocol. Primer sequences and PCR conditions are available on request. Amplicons were analyzed by direct DNA sequencing on an ABI 3130 Genetic Analyzer using the BigDye Terminator version 1.1 Cycle Sequencing Kit. The reported nucleotide and amino acid numbering is relative to the transcription

start site (+1) corresponding to the A of the ATG on the corresponding GeneBank reference sequences.

To establish if each putative mutation was somatic (i.e., tumor specific) or germ-line, the corresponding patient's constitutional DNA was also analyzed when available.

2.11. Bioinformatic Analysis. *In silico* predictions of the putative functional effects of missense mutations in genes coding for TP53, PTEN, and EGFR amplification were determined by PMUT (<http://mmb.pcb.ub.es/PMut/>), PolyPhen (<http://genetics.bwh.harvard.edu/pph/>), and SNAP (<http://cubic.bioc.columbia.edu/services/SNAP/>) programs.

The effect of the intronic variants on splicing was evaluated by SpliceView (<http://bioinfo2.itb.cnr.it/sun/webgene>)

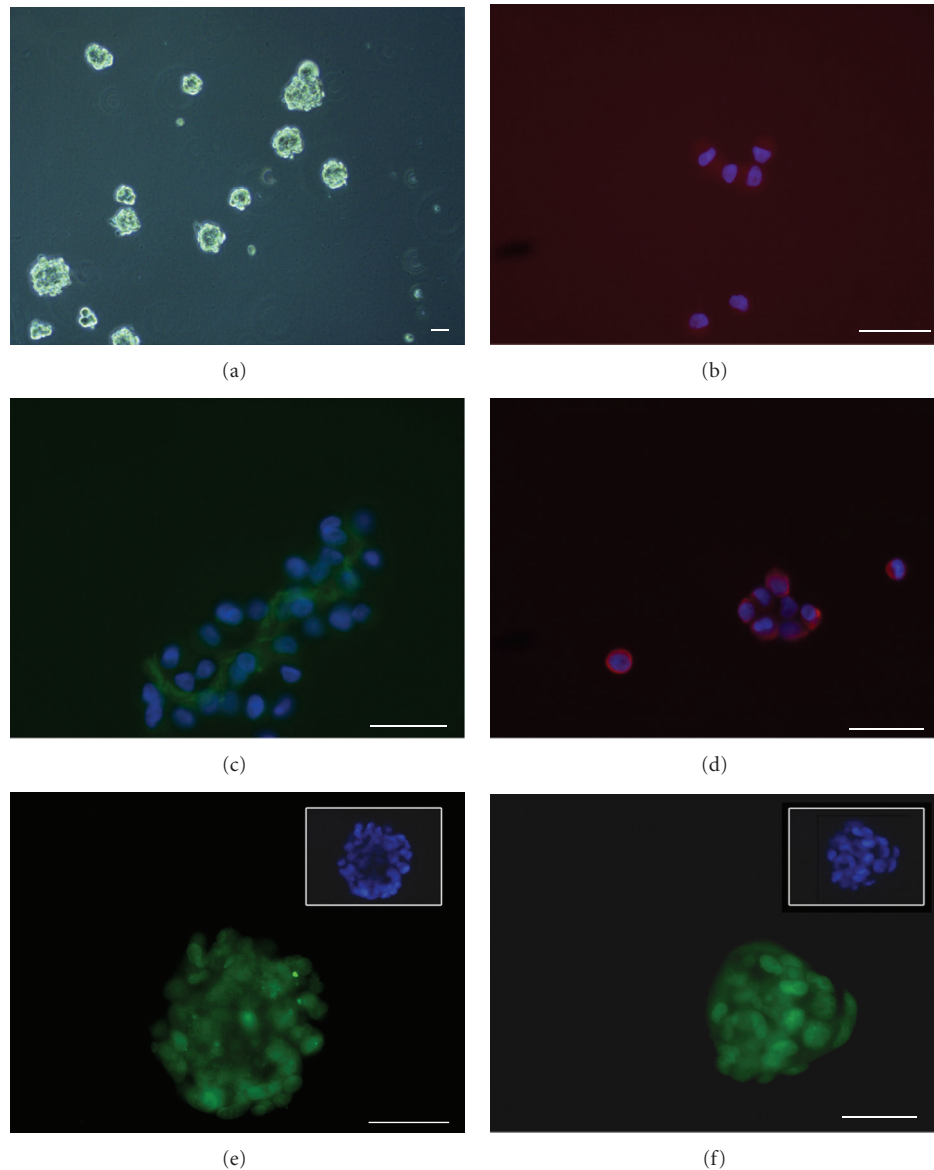


FIGURE 3: Immunofluorescence of NS cultured in serum-free medium. (a) NS. (b) Cytoplasmic expression of CD133. (c) Musashi-1 expression in the cytoplasm. (d) Nestin expression in the cytoplasm. Nuclei are counterstained with DAPI (blue). (e) SOX2 expression in nuclei. (f) REST expression in nuclei. Scale bar 50 μ m.

and NNSplice (<http://biologyhelp.awardspace.com/desc7.php?id=14&type=biotech>) software programs.

2.12. Western Blotting Analysis. Frozen tissue and cultured cells (NS and AC) were homogenized in a lysis buffer (50 mM Tris-HCl, pH 7.4, 150 mM NaCl, 1% v/v Igepal, 2% sodium dodecyl sulfate (SDS), 0.5% sodium deoxycholate, 10 mM EDTA) supplemented with Protease Inhibitor Cocktail (Sigma), 2 mM sodium orthovanadate, and 10 mM sodium fluoride. Tissues were sonicated with three, 10-s bursts. Whole protein extracts were quantified by BCA Protein Assay Kit (Pierce Biotechnology, Rockford, IL, USA) and equal amounts were resolved in 10% SDS-PAGE gels and transferred onto PVDF membranes (Immobilon-

P, Millipore, Bedford, MA). Blots were probed with the antibodies listed in Table 1. Membranes were then incubated with the appropriate HRP-conjugated secondary antibodies and proteins were detected by enhanced chemiluminescence (Millipore). An anti- α -Tubulin antibody was used to normalize sample loading and transfer. Band intensity was quantified by densitometry using NIH Image J software (RSB, NIMH, Bethesda, MD, USA).

3. Results

3.1. Histology. Slices from the 16 tumor samples used for histological analyses were serial to those used for cell culture. The following phenotypic features characterized 4 of the 6

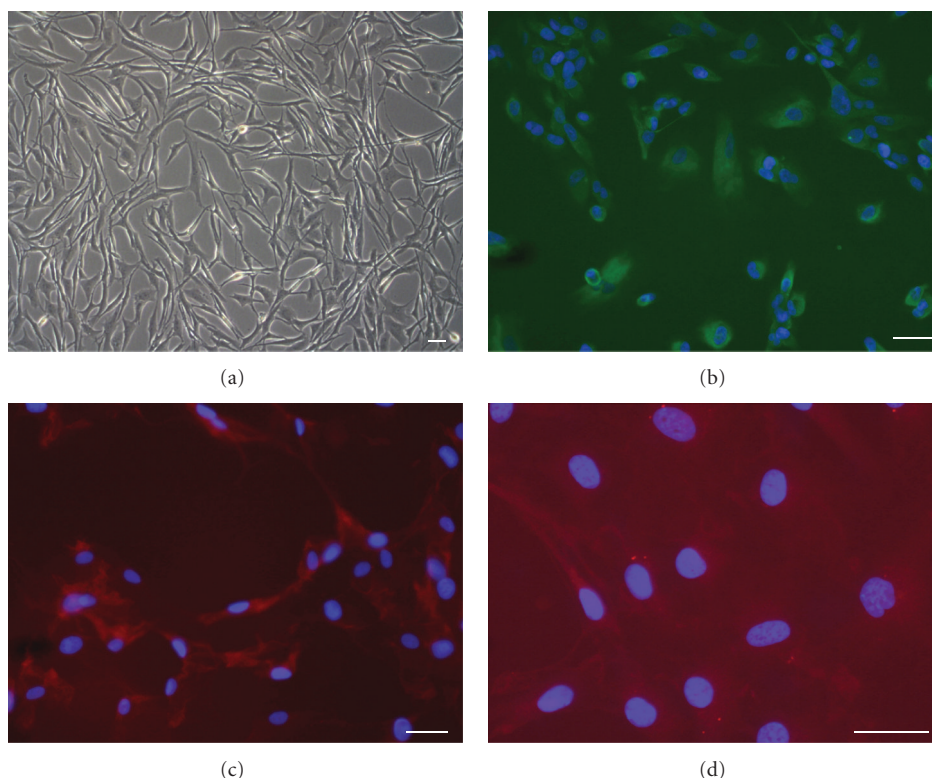


FIGURE 4: Immunofluorescence of AC cultured in serum-containing medium. (a) Monolayer of adherent cells. (b) GFAP expression in the cytoplasm. (c) Cytoplasmic expression of GalC. (d) Cytoplasmic expression of β -III Tubulin. Nuclei are counterstained with DAPI (blue). Scale bar 50 μ m.

samples from which NS generated and 3 of the 9 samples from which AC generated: high cell density, high number of mitoses, a Ki-67/MIB-1 labeling index (LI) between 25% and 30%, circumscribed necroses with pseudo-palisading, high vessel density, and perivascular cuffs of tumor cells (Figure 1).

3.2. Immunohistochemistry of Primary Tumors. Nestin was variably expressed in all GBMs, but its distribution did not completely overlap with that of GFAP. As a matter of fact, Nestin expression was higher than GFAP expression, considering both the number of positive cells and the same cells (Figures 2(a) and 2(b)). SOX2 and REST, which are diffusely expressed in all GBMs, reached the highest intensity in the areas the phenotype of which has been above described and around vessels (Figures 2(c) and 2(d)).

3.3. Immunofluorescence of Primary Tumors (Frozen Sections). As determined by analysis of frozen sections, CD133 and Musashi-1 were sporadically expressed in areas of variable size or in single cells (Figures 2(e) and 2(f)).

3.4. In Vitro Culture Assay. NS and AC were observed in cultures from 6 (CV1, CV7, CV10, CV13, CV17, and CV20) and 9 (CV1, CV2, CV3, CV4, CV6, CV8, CV9, CV10, and CV17) of the 16 samples, respectively (37.5% and 56.3%). Cells derived from CV10 primarily grew as AC, occasionally

forming cell aggregates attached to the culture plate. When CV10 aggregates were transferred to a low-adherent culture plate with DMEM/F-12 medium and mitogens, they gave rise to NS. In cells derived from CV1, in addition to NS, occasional AC were observed when cultured with DMEM/F-12 and mitogens. Alternatively, cultures derived from CV17 developed both NS and AC in their respective media conditions.

NS cultures were verified to contain true BTSCs by assessing their long-term self-renewing ability by population analysis. Cells grown in culture with growth factors proliferated as nonadherent, multicellular spheres (Figure 3(a)), whereas cells grown with serum proliferated as an adherent monolayer with an initial heterogeneous morphology which later became homogeneous with resemblance to fibroblasts (Figure 4(a)) and showing astrocytic, oligodendrocytic, or neuronal differentiation (Figures 4(b)–4(d)). Growth rates of NS and AC are illustrated in Figures 5(a) and 5(b). Figure 5(c) shows the different growth rates between NS and AC of the same cell line.

The subsphere-forming assay performed by limiting dilution demonstrated that the clonogenic efficiency of all NS to form subspheres from individual NS cells was 7–9%.

By differentiation assays NS demonstrated their multipotency showing after 7 days from the addition of 3% serum an astrocytic, oligodendrocytic and neuronal differentiation (Figures 6(a)–6(c)). Upon intracranial transplantation, NS

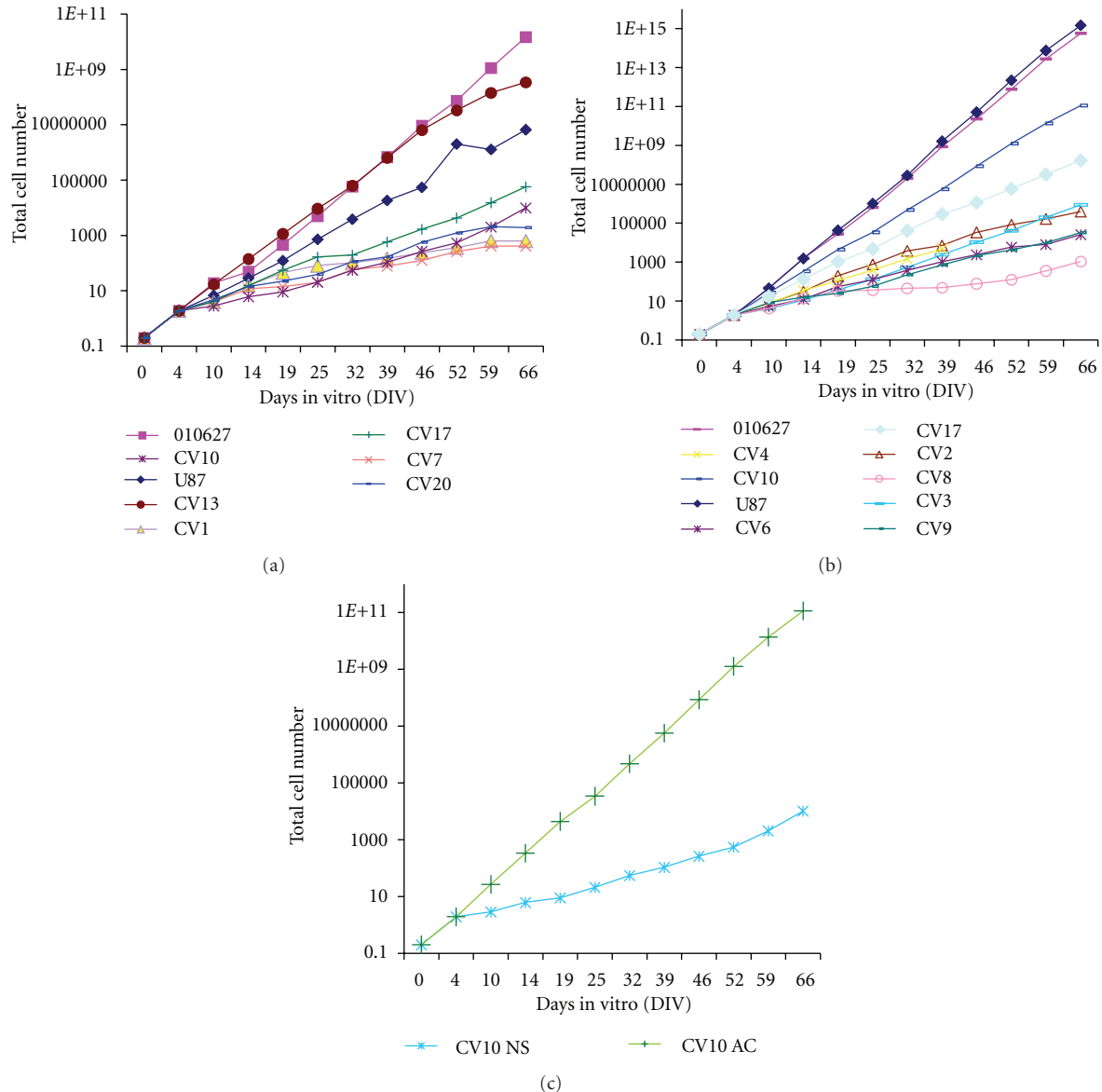


FIGURE 5: Growth rates of NS and AC. (a) Growth curves of NS cultured in serum-free medium supplemented with mitogens from CV1, CV7, CV10, CV13, CV17, CV20, and reference cell lines U87-MG and 010627. (b) Growth curves of AC cultured in serum containing medium from CV2, CV3, CV4, CV6, CV8, CV9, CV10, CV17 (CV1 is not included), and reference cell lines U87-MG and 010627. (c) Comparison between NS and AC curves.

developed tumors in mice, whereas AC did not developed tumors or showed a reduced tumorigenicity in two cases (data not shown), demonstrating that NS populations included true BTSCs. Details of intracranial transplantations will be discussed in a separate manuscript.

3.5. Immunofluorescent Analysis of Cell Lines. NS and AC showed different antigenic expression patterns. Nestin was strongly expressed in NS, along with SOX2 and REST, whereas CD133 and Musashi-1 were only sporadically expressed (Figures 3(b)–3(f)). GFAP was expressed in cells from only one sample (CV7). AC, in contrast, showed decreased Nestin expression and increased GFAP expression when compared with NS. Both CD133 and Musashi-1 expression was almost

completely absent in AC. Nuclear expression of SOX2 and REST was lower in AC when compared to NS.

Comparisons of primary tumors, NS and AC are shown in Table 3. The expression of antigens indicative of stemness was highest in primary tumors and NS, whereas the expression of antigens indicative of differentiation was highest in AC.

3.6. Molecular Genetics. The derivation of NS and AC from the respective primary tumors was confirmed by genotyping of the 13 microsatellite markers used for LOH analysis.

Genetic alterations in primary tumors and in the matched NS or AC are summarized in Table 4. Their frequency is consistent with the primary nature of GBMs. No

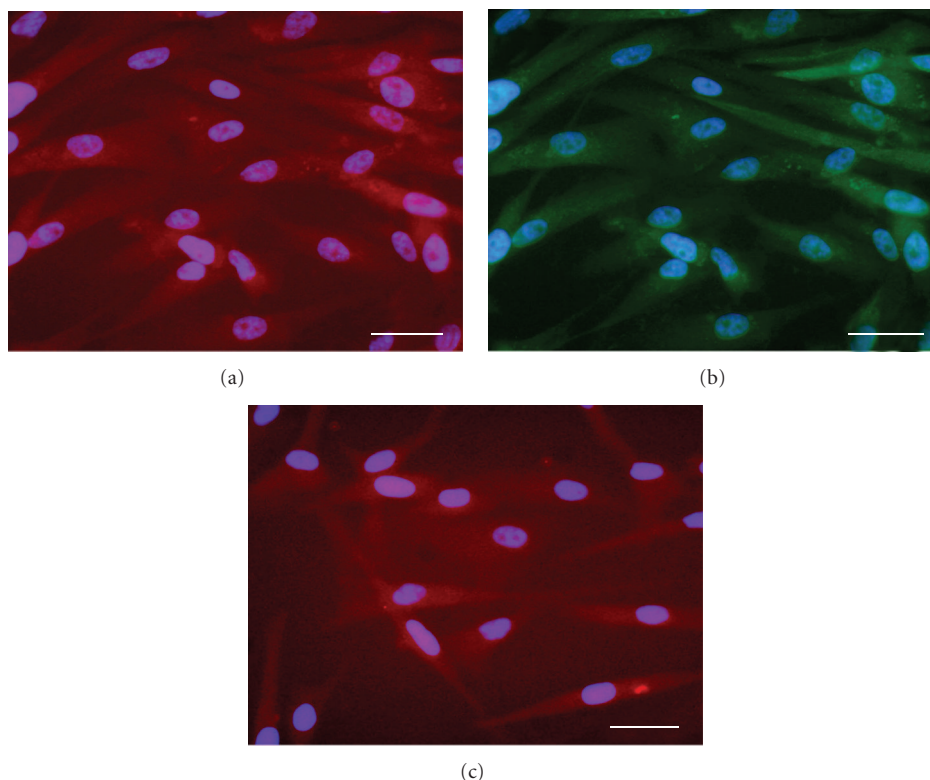


FIGURE 6: Immunofluorescence of differentiation of NS after addition of 3% serum. (a) Cytoplasmic expression of β III-Tubulin (red). (b) Cytoplasmic expression of GFAP (green). (c) Cytoplasmic expression of GalC (red). Nuclei are counterstained with DAPI (blue). Scale bar 50 μ m.

significant differences in the frequency of genetic or epigenetic alterations were observed between primary tumors generating cell lines and those not generating cell lines. In addition, no differences were observed between primary tumors generating NS or AC. LOH on chromosomes 1p, 9p, 10q, 17p, and 19q, EGFR amplification, MGMT promoter hypermethylation as well as PTEN and TP53 mutations was identified with similar frequency in primary tumors and NS, but not in AC. In primary tumors, PTEN mutations were detected in 56.2% of cases, whereas only 31.2% of cases showed TP53 mutations. The TK domain of the gene coding for EGFR was found to be mutated in only one primary tumor (CV6) generating AC. This previously undescribed mutation was a somatic synonymous nucleotide substitution (c.2904C > T, p.F968F). All observed nucleotide sequence variations are reported in Table 5. No point mutations were identified in codons R132 or R172 of IDH1 and IDH2 genes, respectively.

With respect to LOH analysis, the specific spectrum of LOH present in primary tumors was detected only in NS. LOH of 10q was present in all primary tumors, followed by LOH of 9p in 8 of the 16 cases (50%). LOH of 1p, 17p, and 19q was observed only occasionally. The allelic imbalance was partial in all primary tumors and complete in NS (Figure 7). No detectable LOH was identified in AC. In line with these data, MGMT was hypermethylated in 50% of primary tumors and in 63.7% of NS. Remarkably, AC from CV10 showed a molecular profile typical of NS.

3.7. Western Blotting Analysis. Western blotting analysis confirmed a higher prevalence of antigens indicative of stemness in primary tumors and NS when compared to AC, in which antigens indicative of differentiation were more highly expressed. MGMT expression was consistent with the MGMT promoter hypermethylation status (Figure 8(a)). Densitometric analyses of the antigens studied in NS, AC, and the corresponding primary tumors are reported in Figures 8(b) and 8(c).

4. Discussion

One important question is whether GBMs are heterogeneous with respect to their BTSC content. Basically, it has been demonstrated that different subsets of BTSCs with different proliferative, clonogenic, and tumorigenic properties exist in GBMs [3]. Moreover, chemosensitivity of highly infiltrative GBMs has been demonstrated to be associated with a stem cell-like phenotype, that is, with the expression of Nestin, Vimentin, and Musashi-1 [3, 29]. In a study no difference was found among several samples from the same tumor as for their BTSC content [22], but in another study the existence of at least two types of BTSCs from different regions of the same tumor has been demonstrated; they showed different genetic anomalies and tumorigenic potentials, even though the cells were considered to derive from common ancestors [21]. The demonstration of BTSCs largely depends on the technical procedures, but in most studies only approximately

TABLE 3: Primary tumors, NS and AC. Immunohistochemistry and immunofluorescence.

(a)									
Antibodies	FFPE sections								
	CV1	CV7	CV10	CV13	CV17	CV20			
GFAP	+	+	+	+	+	±			
βIII-Tubulin	–	–	+	–	–	–			
GalC	–	–	–	–	–	–			
Nestin	++	++	+	++	++	++			
CD133	–*	–*	±*	±*	±*	+			
Musashi-1	–*	–*	±*	±*	–*	+			
SOX2	++	++	++	++	++	++			
REST	++	++	++	++	++	++			
Antibodies	NS								
	CV1	CV7	CV10	CV13	CV17	CV20			
GFAP	±	+	±	–	–	–			
βIII-Tubulin	–	+	+	–	–	±			
GalC	–	+	±	–	–	±			
Nestin	+	+	+	+	+	±			
CD133	+	+	+	±	–	–			
Musashi-1	+	+	±	±	–	–			
SOX2	+	+	+	+	+	+			
REST	+	+	+	+	+	+			
(b)									
Antibodies	FFPE sections								
	CV1	CV2	CV3	CV4	CV6	CV8	CV9	CV10	CV17
GFAP	++	+	++	+	+	+	+	+	+
βIII-Tubulin	±	–	+	–	–	–	–	–	–
GalC	–	–	–	–	–	–	–	–	–
Nestin	+	+	+	+	+	+	+	+	+
CD133	–*	–*	±*	±*	±*	–*	–	–	–
Musashi-1	–*	–*	±*	±*	–*	–*	–	–	–
SOX2	+	+	+	+	+	+	+	+	+
REST	+	+	+	+	+	+	+	+	+
Antibodies	AC								
	CV1	CV2	CV3	CV4	CV6	CV8	CV9	CV10	CV17
GFAP	+	+	+	+	+	+	+	+	+
βIII-Tubulin	+	+	+	–	±	±	–	–	+
GalC	–	+	+	–	+	±	–	–	+
Nestin	+	+	+	+	+	+	+	+	+
CD133	–	–	+	–	±	–	–	–	+
Musashi-1	±	–	+	–	±	±	–	–	+
SOX2	–	–	–	–	+°	±	+°	+	+°
REST	–	–	–	+	+°	+	+°	–	+°

* Tested by IF on primary tumor frozen sections. °Cytoplasmic staining. +Moderate expression intensity. ++High expression intensity. ± Barely visible. – Negative.

30% of GBMs generate NS [22]. Selecting differently glioma initiating cells, for example by autofluorescence, these can be found in all glioma types [30].

In our GBM series, the development of NS in culture is largely dependent on the occurrence in primary tumors of

what is known as the most malignant phenotype of GMB, composed of small hyperchromatic and rapidly dividing cells, with vessel hyperdensity and circumscribed necroses [23]. In the present study, the most important observation is that the frequency of the genetic and epigenetic alterations

TABLE 4: Frequency of genetic and epigenetic alterations in primary tumors, NS and AC.

Molecular marker	Primary GBM (%)	NS (%)	AC* (%)
LOH 1p, 9p, 10q, 17p, 19q	16 (100)	6 (100)	0 (0)
EGFR amplification	8 (50)	3 (45)	0 (0)
MGMT hypermethylation	9 (50)	4 (66.7)	0 (0)
TP53 mutations	5 (31.2)	3 (50)	0 (0)
PTEN mutations	9 (56.2)	4 (66.7)	2 (22.2)
EGFR mutations	1 (<1)	0 (0)	0 (0)
p.R132 IDH1	0 (0)	0 (0)	0 (0)
p.R172 IDH2	0 (0)	0 (0)	0 (0)

* An exception is CV10 in which NS generated from AC. AC showed the same molecular profile of NS.

TABLE 5: Spectrum of the identified sequence variations.

Gene	CDS variation	AA variation	Location	refSNP ID	Function	Number of heterozygous patients
TP53	IVS3-29C>A ^a	p.?	IVS3	rs17883323		1
	c.215G>C	p.R72P	Exon 4	rs1042522	Functional polymorphism	6
	IVS4+5G>C ^{a,d}	p.?	IVS4	<i>de novo</i>	Splice variant	1
	c.388C>A ^d	p.L130I	Exon 5	<i>de novo</i>	Missense	1
	c.473G>T ^{b,c}	p.R158L	Exon 5		Missense	1
	c.527G>A ^{b,c}	p.C176Y	Exon 5		Missense	1
	c.639A>G ^b	p.R213R	Exon 6	rs1800372	Nonsense	2
	IVS6+31A>G ^a	p.?	IVS6	rs34949160	No splice variant	3
	IVS6+62G>A ^a	p.?	IVS6	rs1625895	No splice variant	7
	IVS6-36G>C ^a	p.?	IVS6	rs17880604	No splice variant	1
	c.713G>A ^{b,c}	p.C238Y	Exon 7		Missense	1
	IVS7-35A>G ^{a,d}	p.?	IVS7	<i>de novo</i>	No splice variant	1
	c.817C>T ^{b,c}	p.R273C	Exon 8	rs1625895	Missense	2
	c.832C>T ^{b,c}	p.P278S	Exon 8		Missense	1
PTEN	c.170_171insT ^c	p.L57fs*5	Exon 3		Frame-shift and stop codon	1
	IVS3+1G>T ^{a,c}	p.?	IVS3		No splice variant	
	c.328C>T ^c	p.Q110*	Exon 5		Stop codon	1
	c.371G>A ^d	p.C124Y	Exon 5	<i>de novo</i>	Missense	1
	c.388C>T ^c	p.R130*	Exon 5		Stop codon	1
	c.395G>A ^c	p.G132D	Exon 5		Missense	1
	c.538T>C ^d	p.Y180H	Exon 6	<i>de novo</i>	Missense	1
	c.541delC ^d	p.L181fs*1	Exon 6	<i>de novo</i>	Frame-shift and stop codon	1
	IVS6+2T>G ^a	p.?	IVS6	<i>de novo</i>	Splice variant	1
	c.754G>A	p.D252N	Exon 7	<i>de novo</i>	Missense	1
	IVS8+32T>G ^a	p.?	IVS8	rs555895	No splice variant	8
	c.954_957delTACT ^c	p.L318fs*2	Exon 8		Frame-shift and stop codon	1
	c.1061C>T ^{d,e}	p.P354L	Exon 9		Missense	1
EGFR	IVS18+19G>A ^a	p.?	IVS18	rs17337107		4
	IVS18+100C>T ^a	p.?	IVS18	rs17290336		2
	IVS19-60T>C ^a	p.?	IVS19	rs10241451		5
	c.2361A>G	p.Q787Q	Exon 20	rs1050171	Nonsense	11
	c.2508C>T	p.R836R	Exon 21	rs17290559	Nonsense	1
	c.2709C>T	p.T903T	Exon 23	rs1140475	Nonsense	6
	c.2904C>T ^d	p.F968F	Exon 24	<i>de novo</i>	Nonsense	1

^aThe numbering of intronic variations is relative to the first (+) or the last (-) nucleotide of the corresponding intron.

^bPreviously reported as somatic mutation in gliomas or glioma cell lines at the International Agency for Research on Cancer (<http://www-p53.iarc.fr/>).

^cPreviously reported in gliomas or glioma cell lines in the Catalogue of Somatic Mutations in Cancer (<http://www.sanger.ac.uk/genetics/CGP/cosmic/>).

^dVariations identified *de novo* in gliomas in the present study.

^eAlready present in the patient's constitutive DNA.

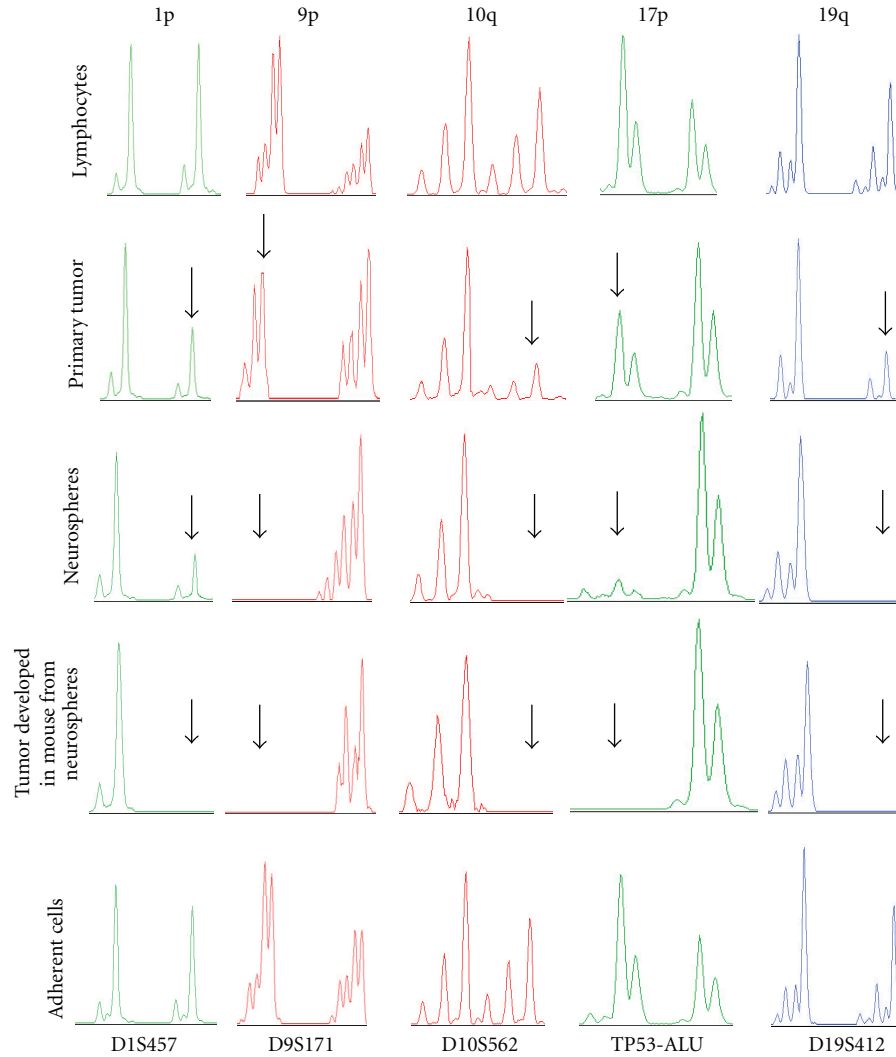


FIGURE 7: Genetic analysis for CV17 primary tumor, NS, AC, and brain tumor developed in mouse after transplantation of CV17 NS. LOH on CV17 primary tumor, NS, AC, constitutive DNA, and on brain tumor developed after NS transplantation into *Nod Scid* mice. Electropherograms show allelic imbalances for the following microsatellite markers: D1S457 (green), D9S171 (red), D10S562 (red), TP53-Alu (green), and D19S412 (blue). For all markers, primary tumor shows a partial allelic imbalance in comparison with the constitutive DNA, which is complete in NS, with the exception of D1S457 and TP53-Alu, and in CV17 mouse brain tumor. Arrows indicate, for each marker, the allelic imbalance in primary tumor, NS and in mouse brain tumor.

is very similar between primary tumors and NS, showing a strong genotypic concordance. This is particularly remarkable in the case of LOH profiles, which are present with the same spectrum in both primary tumors and NS, but not in AC. This observation is consistent with previous data [31]. The allelic imbalance was partial in primary tumors and complete in NS. In AC, no detectable genetic or epigenetic alteration similar to that of the corresponding primary tumor was observed, with the exception of occasional PTEN mutations. The MGMT hypermethylation status and the EGFR amplification status showed a similar frequency between primary tumors and NS, but not between primary tumors and AC. The same is true for the mutation spectrum of TP53 and PTEN genes. In 3 of our cases, both NS and AC developed from the same tumor sample indicating that cells with different potential can coexist in the same tumor. Inter-

estingly, in 1 of these 3 cases, AC generating NS showed the same molecular profile as NS.

The prevalence of Nestin upon GFAP and the expression of stemness antigens in perivascular cuffs and in areas with vessel hyperdensity of primary tumors is in line with the preference of BTSCs for perivascular niches [32–34]. The latter recapitulate normal NSCs and the vasculature of developing nervous system [35, 36]; on the other hand, BTSCs in gliomas mediate vascular proliferation *via* VEGF [37, 38].

The different behavior of NS and AC may be due to showing the former full stemness properties and appearing the latter as the product of cell differentiation. NS could be transformed NSCs from germinal zones, subventricular zone (SVZ), or subgranular zone (SGZ), or from dedifferentiated elements of the astrocytic lineage [39], whereas AC could

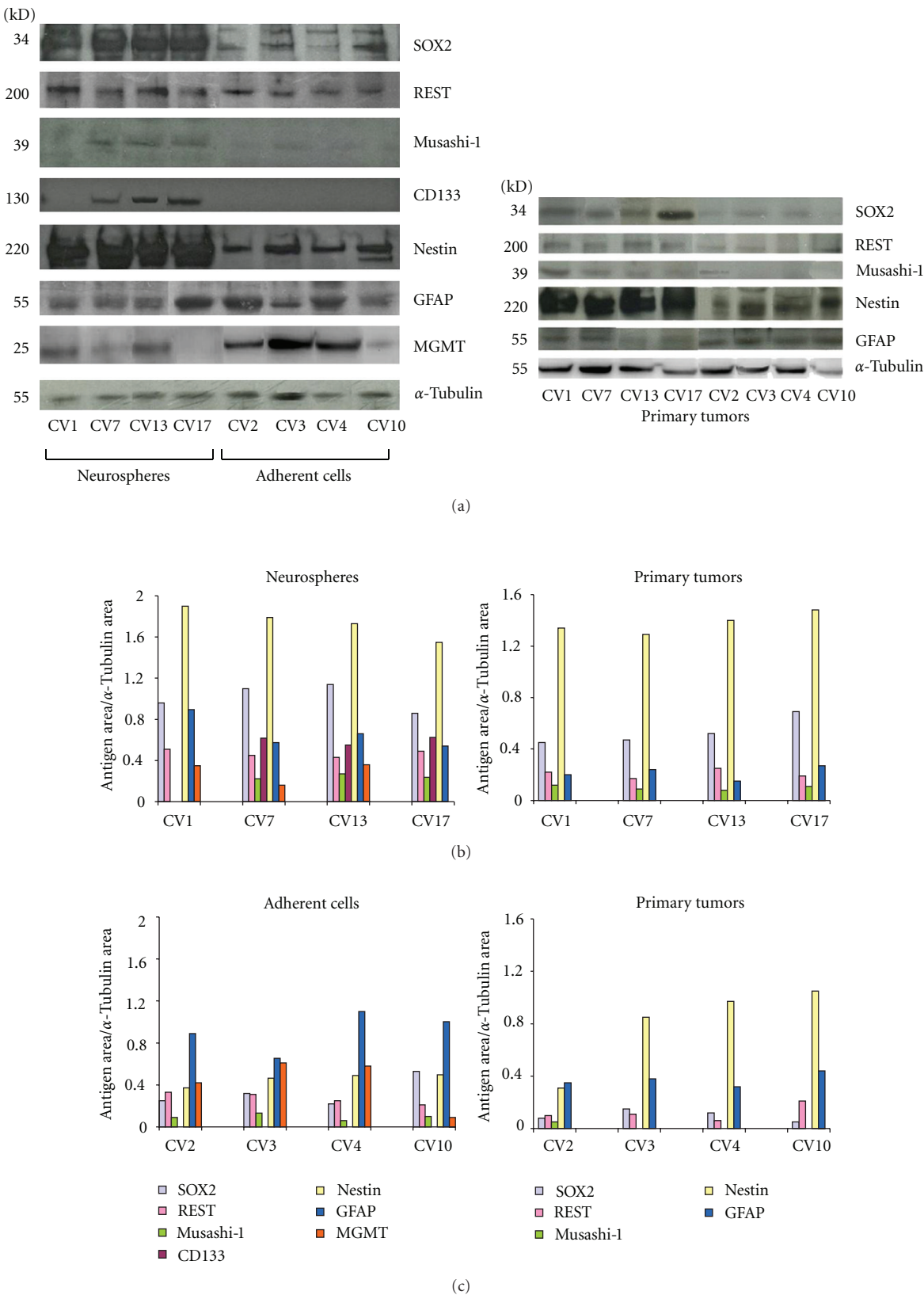


FIGURE 8: Western blotting analysis of the different antigens studied in cell lines (NS and AC) and in primary tumors. (a) Stemness antigens and differentiation antigens prevail in NS and AC, respectively. (b) Densitometric quantification of bands in NS and in the corresponding primary tumors. (c) Densitometric quantification of bands in AC and in the corresponding primary tumors.

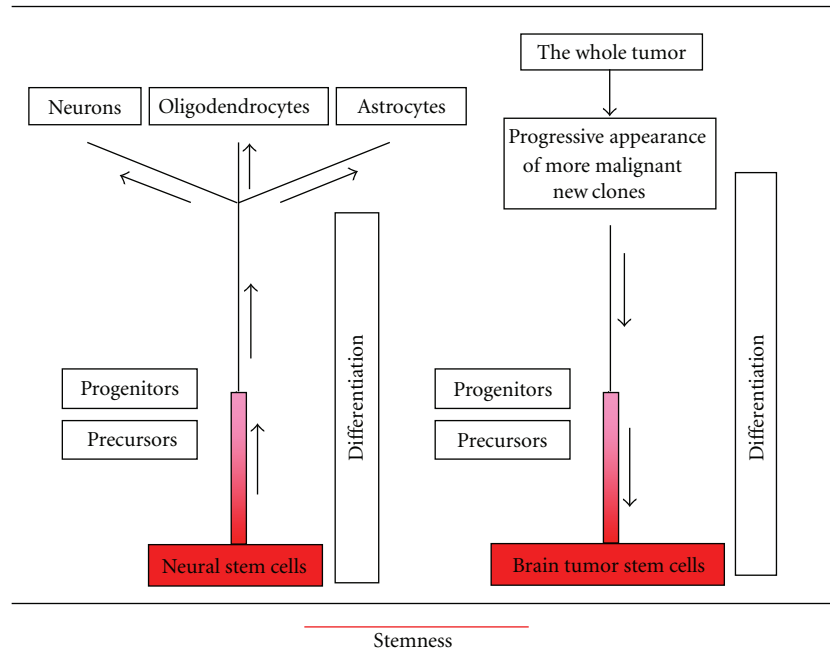


FIGURE 9: Scheme of a hypothetical distribution of stemness during differentiation and dedifferentiation. Stemness decreases from the stage of neural stem cells toward progenitors and adult cells. Conversely, in tumors it increases to a maximum in the stage of brain tumor stem cells.

represent a differentiating cell type. Intermediated behaviors have been observed in our material, as it has been already shown [20].

The generation of NS from a tumor sample mostly when it shows the mentioned phenotype may suggest that BTSCs arise from or are contained in the novel, proliferating and dedifferentiated clones which develop following mutation accumulation or epigenetic events during malignant transformation and substitute the predecessors *via* competitive selection [10]. This hypothesis, previously considered [3, 8, 10, 11], regards dedifferentiated cells as regressed to an embryonic state reacquiring a stem cell-like status. Embryonic regression has been previously invoked, for example, for reactive astrocytes reexpressing Nestin [40, 41].

Our observations concern a very important debated question, that is, the cell composition of a starting tumor tissue. It is not clear whether a major role is played by the occurrence of BTSCs in the tissue or by culture conditions. On the other hand, a clear distinction between NS and AC is still debated concerning self-renewal, clonogenicity and tumorigenicity, and intermediate stages between them exist; terms such as semiadherent cells have been coined for them [20]. This is confirmed by the behavior of CV1, CV10, and CV17 of our series.

Stemness, therefore, might not be a property of a specific cell type, but a status which encompasses the early steps of the cytogenesis. It is conceivable that in the process of differentiation during cytogenesis there is a point, represented by progenitors, beyond which stemness ceases. In the same way, considering the process of tumor cell dedifferentiation from more differentiated stages, through the development of new clones there should be a point beyond which stemness

reappears. From the different stages of differentiation and dedifferentiation, different stemness potentials could be recognized, explaining intermediate properties (Figure 9). A similar problem has been presented and exhaustively discussed in relation to leukemias [42].

The high expression of SOX2 and REST in primary tumors and NS is a stemness property. In our samples, SOX2 not only correlated with the malignancy grade, but it was also overexpressed in the GBM phenotype from which NS could be generated and even amplified as in NS [43]. SOX2 is therefore a proliferation and stemness factor. REST has been shown to display tumor-suppressor activity [44] and oncogenic functions in medulloblastoma [45]. REST is overexpressed in NSC and in medulloblastomas [46, 47]. We did not find in our samples even a slight REST amplification [48]; however, it is overexpressed in the primary tumor phenotype generating NS. The most commonly held position is that REST could maintain stem cell status [49].

Acknowledgments

This study was supported by a grant from Compagnia di San Paolo, Turin, Italy. The authors are deeply grateful to Dr. Rossella Galli and Dr Stefania Mazzoleni for revising the paper and for the animal implantation.

References

- [1] T. Lapidot, C. Sirard, J. Vormoor et al., "A cell initiating human acute myeloid leukaemia after transplantation into SCID mice," *Nature*, vol. 367, no. 6464, pp. 645–648, 1994.
- [2] T. N. Ignatova, V. G. Kukekov, E. D. Laywell et al., "Human cortical glial tumors contain neural stem-like cells expressing

- astroglial and neuronal markers in vitro," *GLIA*, vol. 39, no. 3, pp. 193–206, 2002.
- [3] R. Galli, E. Binda, U. Orfanelli et al., "Isolation and characterization of tumorigenic, stem-like neural precursors from human glioblastoma," *Cancer Research*, vol. 64, no. 19, pp. 7011–7021, 2004.
 - [4] X. Yuan, J. Curtin, Y. Xiong et al., "Isolation of cancer stem cells from adult glioblastoma multiforme," *Oncogene*, vol. 23, no. 58, pp. 9392–9400, 2004.
 - [5] C. D. Stiles and D. H. Rowitch, "Glioma stem cells: a midterm exam," *Neuron*, vol. 58, no. 6, pp. 832–846, 2008.
 - [6] N. Sanai, A. Alvarez-Buylla, and M. S. Berger, "Neural stem cells and the origin of gliomas," *New England Journal of Medicine*, vol. 353, no. 8, pp. 811–822, 2005.
 - [7] Z. Liu, X. Hu, J. Cai et al., "Induction of oligodendrocyte differentiation by Olig2 and Sox10: evidence for reciprocal interactions and dosage-dependent mechanisms," *Developmental Biology*, vol. 302, no. 2, pp. 683–693, 2007.
 - [8] D. Schiffer, L. Annovazzi, V. Caldera et al., "On the origin and growth of gliomas," *Anticancer Research*, vol. 30, no. 6, pp. 1977–1998, 2010.
 - [9] A. L. Vescovi, R. Galli, and B. A. Reynolds, "Brain tumour stem cells," *Nature Reviews Cancer*, vol. 6, no. 6, pp. 425–436, 2006.
 - [10] D. Schiffer, A. Manazza, and I. Tamagno, "Nestin expression in neuroepithelial tumors," *Neuroscience Letters*, vol. 400, no. 1–2, pp. 80–85, 2006.
 - [11] K. Uchida, M. Mukai, H. Okano et al., "Possible oncogenicity of subventricular zone neural stem cells: case report," *Neurosurgery*, vol. 55, no. 4, pp. 977–978, 2004.
 - [12] M. Pollard, K. Yoshikawa, I. D. Clarke et al., "Glioma stem cell lines expanded in adherent culture have tumor-specific phenotypes and are suitable for chemical and genetic screens," *Cell Stem Cell*, vol. 4, no. 6, pp. 568–580, 2009.
 - [13] B. A. Reynolds and A. L. Vescovi, "Brain cancer stem cells: think twice before going flat," *Cell Stem Cell*, vol. 5, no. 5, pp. 466–467, 2009.
 - [14] D. Bexell, S. Gunnarsson, P. Siesjö et al., "CD133+ and nestin+ tumor-initiating cells dominate in N29 and N32 experimental gliomas," *International Journal of Cancer*, vol. 125, no. 1, pp. 15–22, 2009.
 - [15] Y. Kamachi, M. Iwafuchi, Y. Okuda et al., "Evolution of non-coding regulatory sequences involved in the developmental process: reflection of differential employment of paralogous genes as highlighted by Sox2 and group B1 Sox genes," *Proceedings of the Japan Academy B*, vol. 85, no. 2, pp. 55–68, 2009.
 - [16] M. Schmitz, A. Temme, V. Senner et al., "Identification of SOX2 as a novel glioma-associated antigen and potential target for T cell-based immunotherapy," *British Journal of Cancer*, vol. 96, no. 8, pp. 1293–1301, 2007.
 - [17] C. J. Schoenherr and D. J. Anderson, "Silencing is golden: negative regulation in the control of neuronal gene transcription," *Current Opinion in Neurobiology*, vol. 5, no. 5, pp. 566–571, 1995.
 - [18] Y. M. Sun, D. J. Greenway, R. Johnson et al., "Distinct profiles of REST interactions with its target genes at different stages of neuronal development," *Molecular Biology of the Cell*, vol. 16, no. 12, pp. 5630–5638, 2005.
 - [19] J. Lee, S. Kotliarova, Y. Kotliarov et al., "Tumor stem cells derived from glioblastomas cultured in bFGF and EGF more closely mirror the phenotype and genotype of primary tumors than do serum-cultured cell lines," *Cancer Cell*, vol. 9, no. 5, pp. 391–403, 2006.
 - [20] H. S. Günther, N. O. Schmidt, H. S. Phillips et al., "Glioblastoma-derived stem cell-enriched cultures form distinct subgroups according to molecular and phenotypic criteria," *Oncogene*, vol. 27, no. 20, pp. 2897–2909, 2008.
 - [21] S. G. M. Piccirillo, R. Combi, L. Cajola et al., "Distinct pools of cancer stem-like cells coexist within human glioblastomas and display different tumorigenicity and independent genomic evolution," *Oncogene*, vol. 28, no. 15, pp. 1807–1811, 2009.
 - [22] R. Pallini, L. Ricci-Vitiani, G. L. Banna et al., "Cancer stem cell analysis and clinical outcome in patients with glioblastoma multiforme," *Clinical Cancer Research*, vol. 14, no. 24, pp. 8205–8212, 2008.
 - [23] D. N. Louis, H. Ohgaki, and O. D. Wiestler, *WHO Classification of Tumors of the Central Nervous Systems*, International Agency for Research on Cancer (IARC), Lyon, France, 4th edition, 2007.
 - [24] B. A. Reynolds and S. Weiss, "Generation of neurons and astrocytes from isolated cells of the adult mammalian central nervous system," *Science*, vol. 255, no. 5052, pp. 1707–1710, 1992.
 - [25] P. Kabos, M. Ehtesham, A. Kabosova et al., "Generation of neural progenitor cells from whole adult bone marrow," *Experimental Neurology*, vol. 178, no. 2, pp. 288–293, 2002.
 - [26] L. Bissola, M. Eoli, B. Pollo et al., "Association of chromosome 10 losses and negative prognosis in oligoastrocytomas," *Annals of Neurology*, vol. 52, no. 6, pp. 842–845, 2002.
 - [27] M. Mellai, V. Caldera, L. Annovazzi et al., "MGMT promoter hypermethylation in a series of 104 glioblastomas," *Cancer Genomics and Proteomics*, vol. 6, no. 4, pp. 219–227, 2009.
 - [28] M. Esteller, S. R. Hamilton, P. C. Burger et al., "Inactivation of the DNA repair gene O(6)-methylguanine-DNA methyltransferase by promoter hypermethylation is a common event in primary human neoplasia," *Cancer Research*, vol. 59, no. 4, pp. 793–797, 1999.
 - [29] T. C. A. Johannessen, J. Wang, K. O. Skaftnesmo et al., "Highly infiltrative brain tumours show reduced chemosensitivity associated with a stem cell-like phenotype," *Neuropathology and Applied Neurobiology*, vol. 35, no. 4, pp. 380–393, 2009.
 - [30] V. Clément, D. Marino, C. Cudalbu et al., "Marker-independent identification of glioma-initiating cells," *Nature Methods*, vol. 7, no. 3, pp. 224–228, 2010.
 - [31] P. Tunic, L. Bissola, E. Lualdi et al., "Genetic alterations and in vivo tumorigenicity of neurospheres derived from an adult glioblastoma," *Molecular Cancer*, vol. 3, article no. 25, 2004.
 - [32] S. Bao, Q. Wu, S. Sathornsumetee et al., "Stem cell-like glioma cells promote tumor angiogenesis through vascular endothelial growth factor," *Cancer Research*, vol. 66, no. 16, pp. 7843–7848, 2006.
 - [33] C. Calabrese, H. Poppleton, M. Kocak et al., "A perivascular niche for brain tumor stem cells," *Cancer Cell*, vol. 11, no. 1, pp. 69–82, 2007.
 - [34] Q. Shen, Y. Wang, E. Kokovay et al., "Adult SVZ stem cells lie in a vascular niche: a quantitative analysis of niche cell-cell interactions," *Cell Stem Cell*, vol. 3, no. 3, pp. 289–300, 2008.
 - [35] J. H. McCarty, "Cell adhesion and signaling networks in brain neurovascular units," *Current Opinion in Hematology*, vol. 16, no. 3, pp. 209–214, 2009.
 - [36] M. Tavazoie, L. Van der Veken, V. Silva-Vargas et al., "A specialized vascular niche for adult neural stem cells," *Cell Stem Cell*, vol. 3, no. 3, pp. 279–288, 2008.
 - [37] R. J. Gilbertson and J. N. Rich, "Making a tumour's bed: glioblastoma stem cells and the vascular niche," *Nature Reviews Cancer*, vol. 7, no. 10, pp. 733–736, 2007.
 - [38] A. Veeravagu, S. R. Bababeygy, M. Yashar et al., "The cancer stem cell-vascular niche complex in brain tumor formation," *Stem Cells and Development*, vol. 17, no. 5, pp. 859–867, 2008.

- [39] E. L. Jackson and A. Alvarez-Buylla, "Characterization of adult neural stem cells and their relation to brain tumors," *Cells Tissues Organs*, vol. 188, no. 1-2, pp. 212–224, 2008.
- [40] S. S. Magavi, B. R. Leavitt, and J. D. Macklis, "Induction of neurogenesis in the neocortex of adult mice," *Nature*, vol. 405, no. 6789, pp. 951–955, 2000.
- [41] A. Buffo, I. Rite, P. Tripathi et al., "Origin and progeny of reactive gliosis: a source of multipotent cells in the injured brain," *Proceedings of the National Academy of Sciences of the United States of America*, vol. 105, no. 9, pp. 3581–3586, 2008.
- [42] E. Passegué, C. H. Jamieson, L. E. Ailles et al., "Normal and leukemic hematopoiesis: are leukemias a stem cell disorder or a reacquisition of stem cell characteristics?" *Proceedings of the National Academy of Sciences of the United States of America*, vol. 100, no. 1, pp. 11842–11849, 2003.
- [43] L. Annovazzi, M. Mellai, V. Caldera et al., "SOX2 expression and amplification in gliomas and glioma cell lines," *Cancer Genomics and Proteomics*, vol. 8, no. 3, pp. 139–147, 2011.
- [44] T. F. Westbrook, E. S. Martin, M. R. Schlabach et al., "A genetic screen for candidate tumor suppressors identifies REST," *Cell*, vol. 121, no. 6, pp. 837–848, 2005.
- [45] G. N. Fuller, X. Su, R. E. Price et al., "Many human medulloblastoma tumors overexpress repressor element-1 silencing transcription (REST)/neuron-restrictive silencer factor, which can be functionally countered by REST-VP16," *Molecular Cancer Therapeutics*, vol. 4, no. 3, pp. 343–349, 2005.
- [46] X. Su, S. Kameoka, S. Lentz et al., "Activation of REST/NRSF target genes in neural stem cells is sufficient to cause neuronal differentiation," *Molecular and Cellular Biology*, vol. 24, no. 18, pp. 8018–8025, 2004.
- [47] P. Lawinger, R. Venugopal, Z. S. Guo et al., "The neuronal repressor REST/NRSF is an essential regulator in medulloblastoma cells," *Nature Medicine*, vol. 6, no. 9, pp. 826–831, 2000.
- [48] T. Blom, O. Tynninen, M. Puputti et al., "Molecular genetic analysis of the REST/NRSF gene in nervous system tumors," *Acta Neuropathologica*, vol. 112, no. 4, pp. 483–490, 2006.
- [49] X. Su, V. Gopalakrishnan, D. Stearns et al., "Abnormal expression of REST/NRSF and Myc in neural stem/progenitor cells causes cerebellar tumors by blocking neuronal differentiation," *Molecular and Cellular Biology*, vol. 26, no. 5, pp. 1666–1678, 2006.